Received: 10 November 2019 | Revised: 4 August 2020 | Accepted: 6 August 2020

DOI: 10.1002/mus.27043

CLINICAL RESEARCH ARTICLE

MUSCLE&NERVE WILEY

Textural markers of ultrasonographic nerve alterations in amyotrophic lateral sclerosis

Frank Schreiber MSc[1,2] | Cornelia Garz[1,2] | Hans-Jochen Heinze MD[1,2,3,4] | Susanne Petri MD[5] | Stefan Vielhaber MD[1,2,4] | Stefanie Schreiber MD[1,2,4]

[1]Department of Neurology, Otto von Guericke University, Magdeburg, Germany

[2]German Center for Neurodegenerative Diseases within the Helmholtz Association, Magdeburg, Germany

[3]Leibniz Institute for Neurobiology, Magdeburg, Germany

[4]Center for Behavioral Brain Sciences, Magdeburg, Germany

[5]Department of Neurology, Hannover Medical School, Hannover, Germany

Correspondence
Frank Schreiber, Department of Neurology, Otto von Guericke University, Leipziger Strasse 44, 39120 Magdeburg, Germany.
Email: frank.schreiber@med.ovgu.de

Funding information
Stiftung für Medizinische Wissenschaft, Frankfurt/Main, Germany, Grant Number 02728/STV (to S.S. and S.V.).

Abstract

Ultrasound has revealed cross-sectional nerve area (CSA) reduction in amyotrophic lateral sclerosis (ALS), but little is known about the sonographic nerve texture beyond CSA alterations. In a large cohort of 177 ALS patients and 57 control subjects, we investigated the covariance and disease-specific signature of several sonographic texture features of the median and ulnar nerves and their relationship to the patients' clinical characteristics. ALS patients showed atrophic nerves, a loss of the intranerve structures' echoic contrast, elevated coarseness, and a trend toward lower cluster shading compared with controls. A reduction in intranerve echoic contrast was related to longer disease duration and poorer functional status in ALS. Sonographic texture markers point toward a significant reorganization of the deep nerve microstructure in ALS. Future studies will be needed to further substantiate the markers' potential to assess peripheral nerve alterations in ALS.

KEYWORDS

amyotrophic lateral sclerosis, biomarker, nerve ultrasound, sonographic texture, texture analysis

1 | INTRODUCTION

During the last decade peripheral nerve ultrasound has been increasingly applied to patients with amyotrophic lateral sclerosis (ALS). By measuring the cross-sectional nerve area (CSA), nerve ultrasound has emerged as a valuable technique to aid the often challenging differential diagnosis between ALS and ALS mimics, such as multifocal motor neuropathy (MMN).[1-3] MMN is characterized by segmental CSA enlargement. On a group level, ALS is related to smaller nerve CSA in distal and proximal nerve segments; however, there is much overlap of nerve size between ALS and healthy controls, limiting the utility of nerve ultrasound in the diagnostic work-up of ALS patients.[4-7]

Abbreviations: ALS, amyotrophic lateral sclerosis; ALSFRS-R, ALS Functional Rating Scale—Revised; CIDP, chronic inflammatory demyelinating polyneuropathy; CMAP, compound motor action potential; CON, control; CSA, cross-sectional area; DICOM, Digital Imaging and Communications in Medicine; EI, echointensity; FA, forearm; GLCM, gray-level co-occurrence matrix; GLCM AC, autocorrelation parameter, derived from GLCM; GLCM CON, contrast parameter, derived from GLCM; GLCM ENT, entropy parameter, derived from GLCM; GLCM NRG, energy parameter, derived from GLCM; GLCM PRO, cluster prominence parameter, derived from GLCM; GLCM SHA, cluster shade parameter, derived from GLCM; GLRLM, gray-level run-length matrix; GLRLM HGRE, high gray-level run emphasis parameter, derived from GLRLM; LMN, lower motor neuron; LMND, lower motor neuron dominant; MMN, multifocal motor neuropathy; NGTDM, neighborhood gray tone difference matrix; NGTDM CMP, complexity parameter, derived from NGTDM; NGTDM CRS, coarseness parameter, derived from NGTDM; PC, principal component; PCA, principal component analysis; ROI, region of interest; TIF, Tagged Image File; UMND, upper motor neuron dominant; VAR, gray-level variance.

Beyond CSA measures, sonographic texture analysis could have the potential to uncover correlates of the underlying pathological peripheral nerve alterations in ALS. Sonographic texture features of the peripheral nerves could further offer biological insights into disease stage and severity in ALS. This would be especially important as CSA alterations alone do not add any information about the ALS patients' clinical state.[3,4,6,8,9]

However, thus far only a handful of studies evaluated sonographic nerve texture measures beyond nerve CSA in ALS, such as hypoechoic fraction (as a marker of the intranerve fascicular portion),[3,10] fascicle size, vascularization[3] or echointensity, echovariation, and selected gray-level co-occurrence matrix texture parameters.[9] None of those studies found any alterations of these markers in ALS, which may be due to small sample sizes and the consideration of isolated nerve features. Thus, it remains unknown which deep sonographic nerve infrastructure alterations occur in atrophic nerves in ALS and which texture features may best be suited to detect them.

In light of those uncertainties, we conducted a cross-sectional study in a large cohort of ALS patients who underwent nerve ultrasound. We investigated the covariance and disease-specific signature of several sonographic nerve texture features and examined their relationship to the clinical characteristics of the ALS patients.

2 | METHODS

2.1 | Sample

We included ALS patients from two neurological centers (Departments of Neurology at Otto von Guericke University, Magdeburg, and Hannover Medical School, Hannover, Germany) who underwent upper limb peripheral nerve sonography.

ALS diagnosis was based on the revised El Escorial criteria and included patients with definite, probable, laboratory-supported probable, or possible disease.[11] We also included patients presenting with lower motor neuron (LMN) signs only (formerly designated as "suspected ALS"),[12] but carefully excluded LMN ALS disease mimics, such as immune-mediated neuropathies (chronic inflammatory demyelinating polyradiculoneuropathy [CIDP], MMN), applying clinical, laboratory, and electrophysiological criteria according to international diagnostic consensus criteria.[13,14] None of the patients exhibited focal or segmental enlargement of nerve CSAs, as is typically found in MMN or CIDP. ALS phenotypes comprising classic ALS, lower motor neuron–dominant (LMND), and upper motor neuron–dominant (UMND) ALS were classified in line with operational definitions, as specified in a previous study.[6,15]

Overall disease severity was assessed using the ALS Functional Rating Scale—Revised (ALSFRS-R) and statistical analysis also took account of the ALSFRS-R subscores (gross motor, fine motor, bulbar, and respiratory function).[16] Disease duration was defined as time in months between symptom onset and the sonographic measure.

In addition, compound motor action potential (CMAP) amplitude was determined bilaterally with stimulation at the forearm and wrist (median nerve) and at the elbow and wrist (ulnar nerve) at 34°C.

Sonographic examination was also available from a hospital- and community-based cohort of controls. None of the control subjects had any neuromuscular disorders, nor did they display any specific abnormalities on neurological examination.

The study was approved by the local ethics committee (No. 150/09; No. 16/17), and all subjects gave written informed consent.

2.2 | Peripheral nerve ultrasound

Sonographic examinations of all subjects from the two centers were performed between March 2009 and October 2018 at the Department of Neurology, Otto von Guericke University, Magdeburg. Each subject was in a seated position with the investigator facing the participant. Ulnar and median nerve ultrasound of the right and left upper limbs was performed by two ultrasonographers (S.S. and C.G.) not blinded to the diagnosis, using a 12-MHz linear-array probe (High-End LOGIQ 7; GE Healthcare, Chicago, Illinois). Conditions of the sonographic examination (device, device setting, probe) were kept constant over the entire study period. Transverse images were obtained according to our standard protocol of: (i) the median nerve at the midforearm around 10 cm above the retinaculum flexorum; and of (ii) the ulnar nerve at the lower to middle third of the forearm approximately one-half to three-quarters the distance from the medial epicondyle of the humerus to the ulnar styloid process. Peripheral nerve ultrasound is well established locally with very good to excellent intra- and interrater agreements.[6]

The images captured on the ultrasound device were stored as Digital Imaging and Communications in Medicine (DICOM) files with a resolution of 640 × 480 pixels and converted to Tagged Image File (TIF) format with lossless compression for subsequent analyses.

2.3 | Peripheral nerve features

2.3.1 | Cross-sectional nerve area

Images were stored and offline ultrasound analysis was performed by the same physician (S.S.). In each image the respective nerve was delineated as a region of interest (ROI) by continuous manual tracing of the nerve circumference (excluding the hyperechoic epineural rim). The pixels of each nerve ROI were extracted and the nerve cross-sectional area (CSA) was computed.

2.3.2 | Gray-level histogram features

Beyond the CSA, properties were derived from the gray-level histograms to assess the distribution of the pixels' gray-level intensities

(commonly referred to as *first-order statistics features*). The median gray-level value in an ROI was used as a measure of echointensity (EI) and the variation around the mean was captured by the echovariance (VAR).

2.3.3 | Texture features

Although first-order features provide information about the distribution of intensities, they do not give any information about the relative positions of various gray levels within the ROI. These first-order features will not be able to measure whether all low-value gray levels are positioned together, or if they are interchanged with the high-value gray levels. To further investigate these aspects, a selection of properties was derived from matrices relating local gray levels to values in the vicinity (referred to as *second-order texture features*). Markers were derived from the ROIs' respective gray-level co-occurrence matrix (GLCM), gray-level run-length matrix (GLRLM), and neighborhood gray tone difference matrix (NGTDM) with the gray-level intensities quantized into 256 levels.

For the analysis of the nerve cross-sections in this study, changes are expected in the presentation of distributed clusters representing nerve fascicles and the perineural tissue. The feature selection is therefore focused on the detection of changes in the contrast between hypo- and hyperechoic regions, their distribution, and the sharpness of the transition between them, more in line with the study by Yang et al on the textural features of the parotid gland.[17]

Gray-level co-occurrence matrix. The GLCM encodes the frequency with which two pixels with specific gray-level intensities are positioned a specific distance apart from each other in a specified image direction.[18] To decrease sensitivity to image noise and emphasize the expected intranerve features, the interpixel distance was chosen corresponding to the mean fascicular diameters given by Brill and Tyler[19] for the median nerve at the forearm (0.47 mm) and for the ulnar nerve at the forearm (0.38 mm). Consequently the GLCM is normalized, such that the sum of its entries = 1; thus, the individual elements represent the frequency or probability of each combinations to occur in the image. As no directional preference can be assumed for the nerves' interior structure within the transverse plane, the normalized GLCM for the image directions 0°, 45°, 90°, and 135° were averaged. For the resulting matrices, Haralick presented a range of markers to describe texture.[18] Those that were selected have proven useful in the analysis of nonhomogeneous tissues[17]: *contrast* between pixels (GLCM CON); image *autocorrelation* (GLCM AC); *energy*, a measure of the certainty of gray-level co-occurrence (GLCM NRG); *entropy*, the uncertainty of gray-level co-occurrence (GLCM ENT); *cluster shade*, emphasizing locally shadowed areas (GLCM SHA), as well as *cluster prominence*, indicating large local variations in gray level (GLCM PRO).

Gray-level run-length matrix. The run-length parameters describe the coarseness of the image in a given direction.[20] Of the GLRLM, a long-run and short-run emphasis measure can be derived corresponding to larger and smaller details in the image examined. To assess differences between low- and high-level patches in the ultrasound ROIs, believed to roughly represent nerve fascicles and their surrounding tissue, the high gray-level run emphasis[21] (GLRLM HGRE) was calculated.

Neighborhood gray-tone difference matrix. To quantize typical perceptual attributes of texture, markers based on the neighborhood gray-tone difference matrix were developed by Amadasun and King.[22] Of the described markers, the *coarseness* (NGTDM CRS) is used to assess the size of the patterns and the *complexity* (NGTDM CMP) is used to quantify the visual information content (sharp edges, lines, etc).

All features were calculated using the Image Processing Toolbox version 9.4 in MATLAB R2016a (The MathWorks, Natick, Massachusetts) and the Radiomics Toolbox version 1.2 by Vallières et al.[23]

The ROI parameters were checked for side differences (left vs right arm, dominant vs nondominant arm and, in patients with upper limb onset, upper limb onset side vs later affected upper limb side). Details are presented in Table S1 available online.

A few markers showed differences, with significance $P < .05$, but none of them survived Bonferroni adjustment for the 12 multiple comparisons.

Of the total 57 controls and 177 ALS patients, 346 ROIs of ulnar nerves (82 CON, 264 ALS) and 376 of median nerves (75 CON, 301 ALS) were available for the analysis. Not all probands received high-resolutions ultrasound of both limbs due to time constraints in the clinical setting. All images were visually inspected to ensure sufficient image quality; images with observable artifacts were discarded.

To account for correlations between the ROI markers and the demographic variables of age, sex, height, and weight (see Table S2 online), standardized regression residuals were calculated from the raw values and used for the consecutive steps. This step also prevented a potential distortion by the differently scaled ROI variables in the following step.

2.4 | Peripheral nerve features—principal component analysis

Principal component analysis (PCA) was carried out to expose covariation and reduce the redundancy in and dimension of the data set. The standardized regression residuals were tested for normality using one-sample Kolmogorov-Smirnov tests. None of these variables violated the normality assumption at $P = .05$. The standardized regression residuals for the median and ulnar forearm nerve were used to perform a PCA in MATLAB by employing a maximization variance method.

The overall Kaiser-Meyer-Olkin measure of sampling adequacy for this data set provided a value of 0.70, indicating a moderate but acceptable degree of common variance. The transformation for the control data set resulted in total variance explained of 49.7% and 19.2% for the first two principal components, leading to 68.9% explained variability of the original data in this reduced space.

2.5 | Statistical analysis

For group comparisons, general linear models were conducted for demographic variables as dependent variable and group (ALS vs controls) as independent variable. Sex was compared using the chi-square test.

To account for the effect that bilateral measurements provided in most cases two samples of each ROI measure, group comparisons were carried out using linear mixed effects models with the ROI measures as output, group (ALS vs controls) as fixed, and individual patient identifiers as random variable. As for ROI measures, 12 variables were considered, with Bonferroni-corrected $P \leq .05 / 12 = .004$ considered statistically significant. The effect sizes of the group differences detected in the mixed models was calculated using the difference of group means divided by the pooled standard deviation (Cohen's *d* measure). For the mixed model the standard deviation was calculated to include both the variance between individuals as well as the variance of the measurements in the individuals.[24]

In ALS, calculated principal components were correlated using bivariate correlations with the corresponding CMAP amplitude of the same limb. Correlations with the clinical parameters (ALSFRS-R and its subscores, disease duration) were evaluated using averaged bilateral principle component (PC) scores. Because seven clinical and electrophysiological variables were considered in the correlation analysis, Bonferroni-corrected $P \leq .05 / 7 = .007$ was considered statistically significant. Differences between correlations were tested using a double-sided Fisher's *Z* test as implemented with cocor in R software (R Institute for Statistical Computing, Vienna, Austria).[25]

Sample size calculations for a hypothetical, randomized, controlled trial with a 24-month observation period were conducted using a two-sample *t* test, assuming equal standardized residual group means at disease onset, a 50% treatment effect on the reduction of the PC1 score, an approximately linear decline, a two-sided significance of 0.05, and a power of 0.8. Analysis was performed using nQuery winter 2019 release version 8.5.0 software (Statistical Solutions, Cork, Ireland).

3 | RESULTS

3.1 | Sample

The demographics of the control and ALS cohorts as well as their clinical data are listed in Table 1. There were no group differences between controls and ALS with respect to sex and height. However, ALS patients were slightly older and the patients' weight was significantly lower.

3.2 | Peripheral nerve features

Correlation analyses between the nerve features and the four demographic variables are presented in Table S2 online. In both the control and ALS subgroups, individuals were similarly influenced by these variables, as separate within-subgroup correlations did not show differences between their relations (data not shown). Therefore, group differences in age and weight were accounted for by adjusting the derived texture markers for these values for the whole group.

There were significant group differences between controls and ALS patients for the standardized regression residuals of all selected sonographic markers, namely CSA, gray-level histogram features, and texture features (Table 2). Although the observed differences for the median nerve only reached small effect sizes, differences in the ulnar nerve were more pronounced, with medium effect sizes. Nearly all

TABLE 1 Demographics and clinical data of the study sample

	Controls (n = 57)	ALS (n = 177)	Statistics
Age, years	59.4 [9.7]	62.3 [11.6]	**$F(1) = 4.82$, $P = .03$**
Male sex, n (%)	33 (58)	107 (60)	$\chi^2 = 0.11$, $P = .73$
Height, m	1.72 [0.1]	1.71 [0.1]	$F(1) = 0.14$, $P = .71$
Weight, kg	81.4 [16.4]	74.5 [14.4]	**$F(1) = 7.88$, $P = .01$**
Onset site bulbar / upper limb / lower limb, n (%)	—	48 (27) / 69 (40) / 60 (33)	
Classic / LMND / UMND ALS, n (%)	—	95 (56) / 49 (29) / 27 (16)	
ALSFRS-R bulbar subscore		9 (0-12)	
ALSFRS-R fine motor subscore	—	6 (0-12)	
ALSFRS-R gross motor subscore		6 (0-12)	
ALSFRS-R respiratory subscore		10 (0-12)	
ALSFRS-R total score	—	32 (7-47)	
Disease duration, months	—	33.5 (2.3-120)	

Note: Data expressed as mean [standard deviation] or median (range), unless noted otherwise. $P \leq .05$ considered statistically significant, with significant group differences indicated in bold.

Abbreviations: ALSFRS-R, ALS Functional Rating Scale—Revised; LMND, lower motor neuron dominant; n, number of subjects; UMND, upper motor neuron dominant.

TABLE 2 Peripheral nerve features in controls and ALS

	Med FA controls	Med FA ALS	Med FA statistics	Uln FA controls	Uln FA ALS	Uln FA statistics
CSA	8.6 [1.4]	8.0 [1.4]	F(1) = 1.71, *P* = .192, *d* = 0.13	7.0 [1.3]	5.9 [1.4]	**F(1) = 18.90, P < .001**, d = 0.42**
EI	88.8 [23.1]	83.0 [21.4]	*F*(1) = 1.63, *P* = .202, *d* = 0.17	93.4 [19.3]	79.3 [19.6]	**F(1) = 21.13, P < .001**, d = 0.47**
VAR	1212 [388]	1104 [331]	**F(1) = 8.14, P = .004**, d = 0.29**	1108 [314]	895 [272]	**F(1) = 41.79, P < .001**, d = 0.51**
GLCM AC	9350 [4108]	8223 [3903]	*F*(1) = 2.27, *P* = .13, *d* = 0.19	9964 [3794]	7437 [3350]	**F(1) = 22.24, P < .001**, d = 0.49**
GLCM CON	2172 [737]	1992 [640]	*F*(1) = 7.43, *P* = .007*, *d* = 0.27	2040 [571]	1669 [540]	**F(1) = 37.65, P < .001**, d = 0.47**
GLCM ENT	8.72 [0.24]	8.64 [0.23]	F(1) = 4.29, *P* = .039*, *d* = 0.21	8.55 [0.25]	8.32 [0.27]	**F(1) = 34.30, P < .001**, d = 0.51**
GLCM NRG	1.99×10^{-4} [5.25×10^{-5}]	2.16×10^{-4} [5.43×10^{-5}]	*F*(1) = 3.45, *P* = .064, *d* = 0.19	2.34×10^{-4} [6.27×10^{-5}]	2.96×10^{-4} [9.25×10^{-5}]	**F(1) = 25.57, P < .001**, d = 0.43**
GLCM PRO	2.19×10^{7} [1.43×10^{7}]	1.75×10^{7} [1.09×10^{7}]	**F(1) = 8.27, P = .004**, d = 0.27**	1.83×10^{7} [1.27×10^{7}]	1.17×10^{7} [7.70×10^{6}]	**F(1) = 33.54, P < .001**, d = 0.47**
GLCM SHA	65 384 [46 879]	52 890 [36 684]	*F*(1) = 5.58, *P* = .019*, *d* = 0.21	58 122 [50 135]	41 206 [29 323]	**F(1) = 16.08, P < .001**, d = 0.33**
GLRLM HGRE	10 745 [4380]	9475 [4056]	*F*(1) = 3.10, *P* = .079, *d* = 0.22	11 358 [4071]	8485 [3511]	**F(1) = 27.18, P < .001**, d = 0.54**
NGTDM CMP	67 404 [25 036]	60 538 [21 962]	*F*(1) = 7.28, *P* = .007*, *d* = 0.28	59 436 [16 737]	47 792 [18 846]	**F(1) = 26.00, P < .001**, d = 0.48**
NGTDM CRS	0.0113 [0.00219]	0.0119 [0.00225]	*F*(1) = 1.40, *P* = .237, *d* = 0.11	0.013 [0.00246]	0.015 [0.0027]	**F(1) = 9.77, P = .002**, d = 0.30**

Note: For reasons of illustration, mean [standard deviation] of the extracted *raw value* for each ROI parameter is given. *Statistics* refers to group comparison of standardized regression residuals adjusted for age, sex, height, and weight. Significant group differences are indicated in bold. Cohen's *d* is given as a measure of effect size.

**P* ≤.05.

***P* value considered significant after Bonferroni adjustment (ie, *P* ≤ .05 / 12 = .004).

Abbreviations: ALS, amyotrophic lateral sclerosis; CSA, cross-sectional nerve area; EI, echointensity; FA, forearm; GLCM AC, CON, ENT, NRG, PRO, SHA, autocorrelation, contrast, entropy, energy, cluster prominence, and cluster shade parameters derived from gray-level co-occurrence matrix; GLRLM HGRE, high gray-level run emphasis parameter derived from gray-level run-length matrix; Med, medial; NGTDM CMP, CRS, complexity, and coarseness parameters derived from neighborhood gray-tone difference matrix; Uln, ulnar; VAR, gray-level variance.

sonographic measures, except GLCM NRG and NGTDM CRS, yielded greater values in the control group compared with the ALS group. Refer to Figure S1 online for illustrations of the individual features.

3.3 | Peripheral nerve features—principal component analysis

There were two components extracted from the PCA of the standardized regression residuals of all sonographic markers adjusted for age, sex, height, and weight. The corresponding factor loads are given in Table 3. The first principal component, PC1, was loaded by VAR, GLCM contrast, and GLCM cluster prominence. Larger values of PC1 indicate high gray-level differences and contrast within the nerve ROIs, pointing toward preserved echoic differences of the intranerve structures. PC2 was positively loaded by CSA and negatively by GLCM energy and NGTDM coarseness, indicating that higher values of PC2 are driven by larger CSA with a display of finer intranerve structures. ROIs with small, median, and large PC values are displayed in Figure 1 to illustrate the emphasis of every factor.

TABLE 3 Principal component analysis—factor loads

Input variable	PC1	PC2
CSA	0.10	0.49#
EI	0.24	0.11
VAR	0.37#	−0.16
GLCM AC	0.26	0.10
GLCM CON	0.33#	−0.12
GLCM ENT	0.26	0.39
GLCM NRG	−0.31	−0.41#
GLCM PRO	0.44#	−0.26
GLCM SHA	0.31	−0.34
GLRLM HGRE	0.28	0.07
NGTDM CMP	0.30	−0.16
NGTDM CRS	−0.02	−0.41#
Variance explained	49.7%	19.2%

#The three variables with the highest absolute loads for each PC.
Abbreviations: CSA, cross-sectional nerve area; EI, echointensity; GLCM AC, CON, ENT, NRG, PRO, SHA, autocorrelation, contrast, entropy, energy, cluster prominence, and cluster shade parameters derived from gray-level co-occurrence matrix; GLRLM HGRE high gray-level run emphasis parameter derived from gray-level run-length matrix; NGTDM CMP and CRS, complexity and coarseness parameters derived from neighborhood gray-tone difference matrix; PC, principal component; VAR, gray-level variance.

Group comparisons between controls and ALS for the principal components (PC1-PC2) are displayed in Figure 2. The contrast-driven component PC1 was significantly lower in the median and ulnar nerves in ALS compared with controls (Med FA: $F(1) = 9.45$, $P = .002$, $d = 0.32$; Uln FA: $F(1) = 54.01$, $P < .001$, $d = 0.61$), indicating a loss of echoic contrast within the nerves' area in ALS. In addition, the ulnar nerves in ALS scored lower with regard to PC2 (Med FA: $F(1) = 0.02$, $P = .89$, $d = 0.01$; Uln FA: $F(1) = 4.43$, $P = .036$, $d = 0.20$), pointing toward smaller CSAs and coarser intranerve structures in the ulnar nerve.

In ALS, there was a significant negative correlation between PC1 and disease duration in the median nerve (Figure 3A), whereas, for the ulnar nerve, the significance did not survive the Bonferroni adjustment (Figure 3D). These findings suggest that the echoic contrast within the studied nerves is diminished during the course of the disease. There were positive correlations with medium effect sizes between PC1 and the ALSFRS-R total score, its fine motor subscore, the gross motor subscore (median nerve rho = 0.31, $P < .001$; ulnar nerve rho = 0.31, $P < .001$), as well as correlations with small effect sizes with the respiratory subscore (median nerve rho = 0.23, $P = .004$; ulnar nerve rho = 0.19, $P = .023$). There were, however, no significant correlations between PC1 and the bulbar subscore. This indicates that patients with better preserved echoic contrasts in the median and ulnar nerves tend to score higher on the respective ALSFRS-R scores (median nerve shown in Figure 3B and C and ulnar nerve in Figure 3E and F). A list containing all results of the correlation analysis is given in Table S3 online.

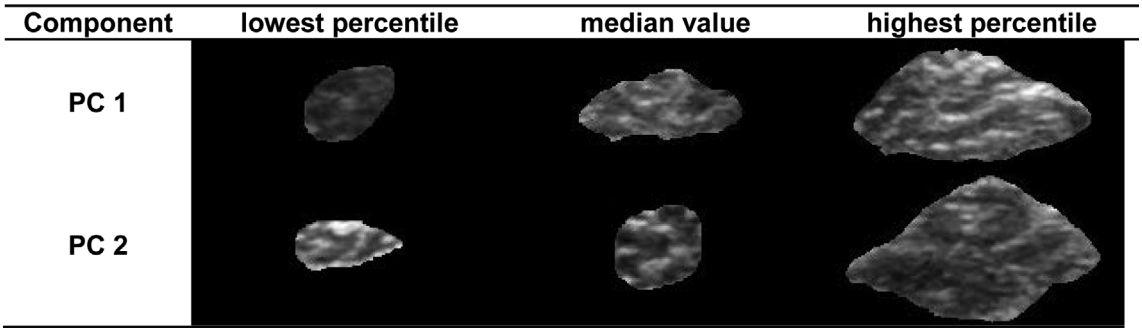

FIGURE 1 Illustration of principal component emphasis. The emphasis of the calculated set of principal components is illustrated by a display of examples from the lowest and the highest percentiles, as well as one with the median parameter value. Larger values of PC1 indicate high gray-level differences and contrast within the nerve regions of interest, pointing toward preserved echoic differences of the intranerve structures. Greater PC2 values are driven by larger cross-sectional area with a display of finer intranerve structures

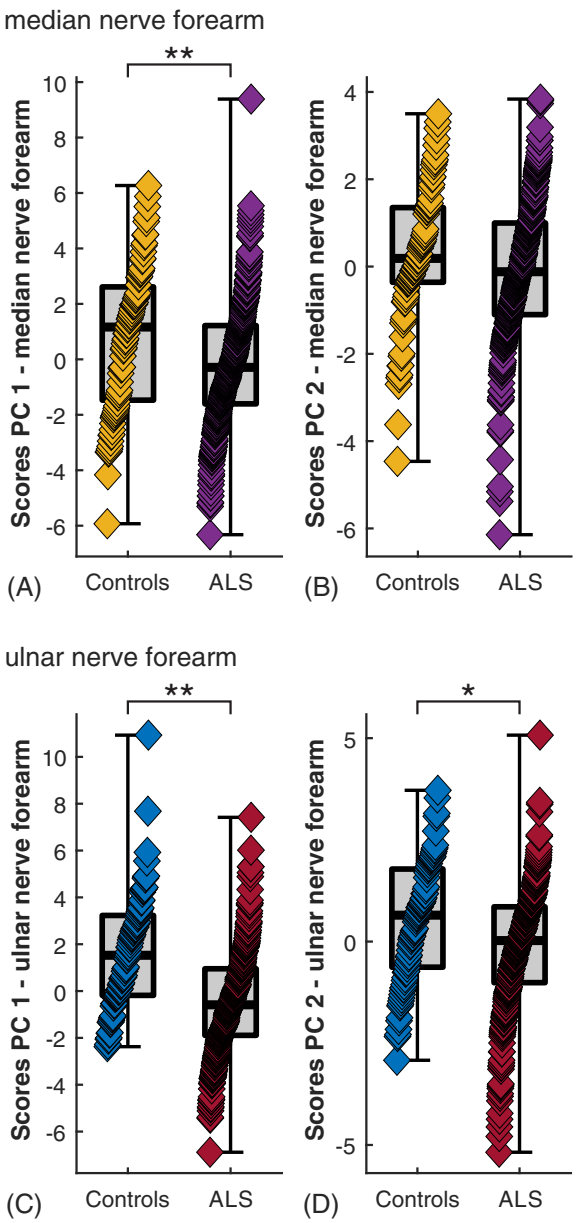

FIGURE 2 Principal components of sonographic measures in controls and ALS patients. Calculated principal components (PC1) for median nerve (upper row) and ulnar nerve (lower row) for controls and ALS patients. As two principal components were considered per nerve, a Bonferroni-corrected $P \leq .05 / 2 = .025$ was considered statistically significant. ALSFRS-R, ALS Functional Rating Scale—Revised; FA, forearm. $^{*}P < .05$, $^{**}P < .025$ [Color figure can be viewed at wileyonlinelibrary.com]

In translating these findings to the context of a randomized, controlled clinical trial with a 24-month observation period, a sample size calculation was carried out to have an 80% chance ($\alpha = 0.05$) of detecting a 50% therapy effect on PC1 score decline in the ulnar and median nerves, which corresponds to a decreased mean decline from −0.85 to −0.43 per year for the ulnar nerve and from −0.41 to −0.21 per year for the median nerve. The necessary size of each trial arm is estimated as 110 patients (ulnar nerve) and 515 patients (median nerve).

4 | DISCUSSION

ALS patients showed atrophic nerves, a loss of the intranerve structures' echoic contrast, elevated coarseness, and a trend toward lower cluster shading compared with controls. Reduction of intranerve echoic contrast seems to be a marker of ongoing disease and poorer overall functional status in ALS. Sonographic texture markers thus point toward a significant reorganization of the deep nerve microstructure, and future studies should aim to further substantiate their potential to assess peripheral nerve alterations in ALS.

Although most studies have focused on usage of CSA as a well-established nerve ultrasound biomarker in ALS,[1,6,26,27] our study has made the case that there is a significant amount of information hidden in the histogram and texture of the cross-sectional nerve image that is still underutilized if not neglected. Our findings point toward significant texture alterations in ALS that, interestingly, do not necessarily covary with the nerve CSA. Texture features thus go beyond the previously established decline of the nerve CSA in ALS and may be a hidden driver behind the large variance reported in several nerve ultrasound studies in ALS.[1,5,6]

Alterations of the nerve texture features most likely reflect the nerves' structural reorganization during the course of disease comprising the loss of large myelinated fibers and axonal degeneration.[28,29] The observed effect of decreased PC1 levels in ALS patients, which indicates a loss of the intranerve echoic contrast, may mirror myelinated fiber and axon reduction. These pathological processes most likely diminish the distinct hypoechoic appearance of the nerve fascicles compared with the surrounding hyperechoic connective tissue,[30] and thus the nerves' contrast. Additional studies combining histopathological and ultrasound examination will be necessary to derive a more profound understanding of the relation between the pathological changes in the nerve tissue and their manifestation in the observed ultrasound texture and derived parameters.

The results of this study point toward a clear correlation between the intranerve echoic contrast as assessed by PC1 and clinical variables such as disease duration, ALSFRS-R total score, and its subscores. The texture markers may thus be superior to nerve CSA in terms of mirroring patients' functional state. This is of pivotal importance when it comes to the selection of indicators to assess the success of therapeutic or interventional trials. Longitudinal studies are necessary to evaluate whether the trajectories of nerve texture features during the ALS disease course possess a potential to aid in the prediction of the patient's prognosis.

The results of the power analyses indicate that the presented compound texture score PC1 may prove useful, especially in the ulnar nerve at the forearm, if employed as additional inclusion parameters in therapeutic trials. However, additional longitudinal studies are needed to verify the assumption of a linear decline of the PC1 over the disease duration.

The reported difference in CSA is in line with several nerve ultrasound studies in ALS.[4-6,9,31,32] Ríos-Días et al also compared the EI and VAR in the median nerves of a smaller ALS cohort and found only a trend-level difference in those markers compared with controls.

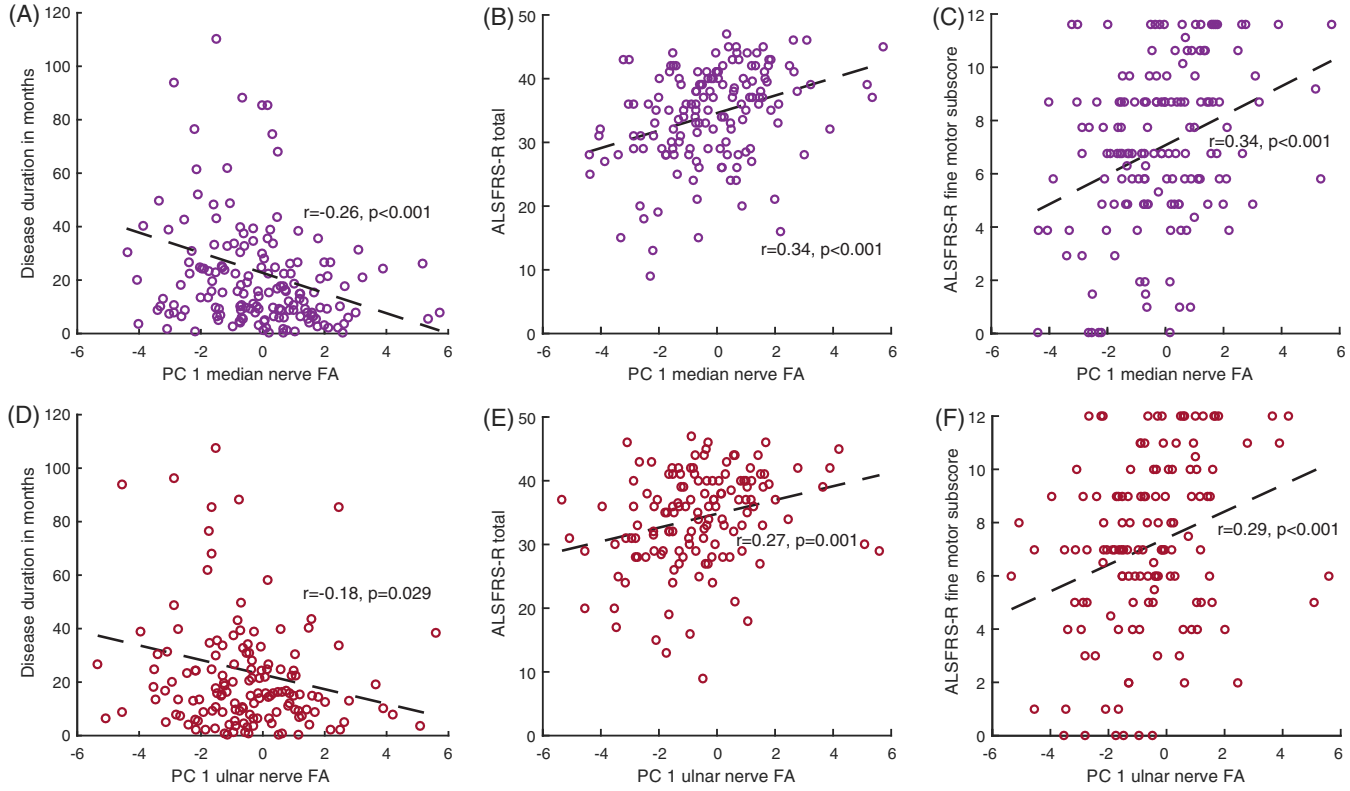

FIGURE 3 Correlations of PC1 with disease durationALS Functional Rating Scale—Revised (ALSFRS-R) total score, and its fine motor subscore. The contrast-driven PC1 for the median (top row) and ulnar nerve (bottom row) sites display significant correlations with disease duration (A, D), ALSFRS-R total score (B, E), and its fine motor subscore (C, F). The positive correlations indicate that patients with better-preserved echoic contrasts tended to score higher on ALSFRS-R scores. The negative correlations with disease duration indicate that the values for PC1 decrease as echoic contrasts decrease over the course of the disease. The relation between PC1 for the median nerve (A) and disease duration reached significance after Bonferroni adjustment, whereas significance did not survive the adjustment for the ulnar nerve (D) [Color figure can be viewed at wileyonlinelibrary.com]

Accordingly, the EI differences did not reach a significant level in the median nerves of our much larger cohort as well, whereas EI was significantly decreased in the ulnar nerves of our ALS sample. However, we found a significant difference in the median and ulnar nerves' VAR, even after Bonferroni adjustment and correction for the aforementioned demographic variables.

Martínez-Paya and colleagues applied a selection of GLCM markers chosen for their potential to detect muscular changes in ALS[33] to the median nerve of ALS patients and controls[9] and found no difference in their GLCM-derived parameters. We believe that the application of markers that are suitable to study changes in muscles are not necessarily best suited to the examination of nerves. Nerve fascicles are much less numerous than muscle fibers and do not exhibit a periodic pattern within the small nerve area.[30] We thus set out to examine markers that have been successfully applied to tissue with a less regular structure such as, for example, the parotid gland, as described by Yang et al.[17]

Moreover, for the GLCM-based markers the choice of the inter-pixel distance for the calculation of the GLCM is of paramount importance. The value of one pixelwidth, chosen in previous studies,[9,33] signifies that the intensity values of directly neighboring pixels are compared in the ensuing analysis. This makes the algorithms most sensitive to detect changes on the scale given by the distance between the pixels (dependent on device resolution, frequency and depth settings, typically in the range of 10 to 50 μm). To make our analysis sensitive to changes on an appropriate anatomically motivated scale we chose to use the mean fascicular diameters as given for healthy controls by Brill and Tyler.[19] The markers derived from the resulting GLCM should be better suited to detect deviations from these features on this scale. This difference in technique and the fact that in our study we were able to utilize the information of a larger sample of ALS patients with a longer disease duration, most likely explains the differences in the results for GLCM markers for the median nerve between our study and the one performed by Martínez-Paya et al.[9]

Although this study offers valuable insight into texture characteristics of peripheral nerve alterations in ALS, it has some limitations. The control and ALS subgroups within this study have different sample sizes and display differences in some demographic parameters, most notably age. However, it was shown that those differences can be accounted for by adjustment for these parameters, as both subgroups display similar correlations with regard to those variables.

The group differences between ALS patients and controls for the texture parameters rise to significance with medium effect sizes for

the ulnar nerve measurements, but conversely in the median nerve only VAR, GLCM PRO, and NGTDM CMP reach significant differences with small effect sizes (Figure 2 and Table 2). The presented correlations in Figure 3 also reach small to medium effect sizes for median and ulnar nerve. These subtle findings, made on group level of a large cohort, most likely limit the future usability as biomarkers, unless substantiated in follow-up studies that show additional advantages.

The algorithms described here were calculated offline, as they are not yet implemented on commercially available ultrasound devices. Because the algorithms are of low complexity, their online evaluation is not only possible, but will most likely be included by device manufacturers as soon as there is sufficient interest in them. Second, settings on the single device used for recording were kept constant between patients to ensure consistency.

Modern ultrasonic transducers use increasingly higher frequencies which will enable higher resolution imaging of the peripheral nerves. In this study we calculated the normalized GLCM matrices not with respect to the pixels' immediate neighbor, but with respect to a distance that corresponds to the median fascicle diameter in controls at the nerve site. We chose this coarser, but physiologically meaningful scale for our analysis to detect deviations, thereby deliberately disregarding finer details in the image. Nerve images taken on higher resolution devices will provide even finer details that will also not affect the analysis, if the interpixel-distance is adjusted as suggested. Our own preliminary results indicate that deviations between parameters calculated for images with higher resolutions are minute (data not shown), if the other preprocessing parameters are held constant.

Echotexture analysis is also likely dependent on device- and manufacturer-specific parameters (probe/beam width, despeckle functions, compression/enveloping of the data, etc), which may present a significant hurdle to the comparison and widespread integration of these parameters. Future studies have to be conducted to identify such standardized quantitative markers that are as robust as possible with regards to the wide range of devices and device-specific settings.

In the future, texture markers may also prove valuable to examine the nerves of patients with more complex diseases of the peripheral nervous system, such as Charcot-Marie-Tooth disease (CMT1) with an inflammatory component or CIDP without active inflammation.[34-36] Sonographic texture markers may serve as a monitoring variable for the characterization of the time course of fascicular and deep nerve microstructure changes in those complex disorders.

Our results point to the potential of sonographic texture markers to assess deep microstructure alterations of the peripheral nerves in ALS. Future studies and technical developments will be needed to determine whether those markers can eventually become part of routine nerve ultrasound clinical practice.

ACKNOWLEDGMENTS

We thank Beryl Darrah for meticulous language editing throughout the manuscript; Anne-Katrin Baum, Department of Neurology, Otto von Guericke University, Magdeburg, Germany, for technical assistance; and Christa Sobetzko, Department of Neurology, Otto von Guericke University, Magdeburg, Germany, for data collection. Open access funding enabled and organized by Projekt DEAL.

CONFLICT OF INTEREST

The authors declare no potential conflicts of interest.

ETHICAL PUBLICATION STATEMENT

We confirm that we have read the Journal's position on issues involved in ethical publication and affirm that this report is consistent with those guidelines.

ORCID

Frank Schreiber https://orcid.org/0000-0002-9484-8613
Susanne Petri https://orcid.org/0000-0002-9783-8584
Stefanie Schreiber https://orcid.org/0000-0003-4439-4374

REFERENCES

1. Grimm A, Decard BF, Athanasopoulou I, Schweikert K, Sinnreich M, Axer H. Nerve ultrasound for differentiation between amyotrophic lateral sclerosis and multifocal motor neuropathy. *J Neurol.* 2015;262:870-880.
2. Loewenbruck KF, Liesenberg J, Dittrich M, et al. Nerve ultrasound in the differentiation of multifocal motor neuropathy (MMN) and amyotrophic lateral sclerosis with predominant lower motor neuron disease (ALS/LMND). *J Neurol.* 2016;263:35-44.
3. Goedee HS, van der Pol WL, van Asseldonk J-TH, et al. Diagnostic value of sonography in treatment-naive chronic inflammatory neuropathies. *Neurology.* 2017;88:143-151.
4. Cartwright MS, Walker FO, Griffin LP, Caress JB. Peripheral nerve and muscle ultrasound in amyotrophic lateral sclerosis. *Muscle Nerve.* 2011;44:346-351.
5. Nodera H, Takamatsu N, Shimatani Y, et al. Thinning of cervical nerve roots and peripheral nerves in ALS as measured by sonography. *Clin Neurophysiol.* 2014;125:1906-1911.
6. Schreiber S, Abdulla S, Debska-Vielhaber G, et al. Peripheral nerve ultrasound in amyotrophic lateral sclerosis phenotypes. *Muscle Nerve.* 2015;51:669-675.
7. Schreiber S, Vielhaber S, Schreiber F, Cartwright MS. Peripheral nerve imaging in amyotrophic lateral sclerosis. *Clin Neurophysiol.* 2020;131(9):2315–2326.
8. Schreiber S, Dannhardt-Stieger V, Henkel D, et al. Quantifying disease progression in amyotrophic lateral sclerosis using peripheral nerve sonography. *Muscle Nerve.* 2016;54:391-397.
9. Ríos-Díaz J, Del Baño-Aledo ME, Tembl-Ferrairó JI, Chumillas MJ, Vázquez-Costa JF, Martínez-Payá JJ. Quantitative neuromuscular ultrasound analysis as biomarkers in amyotrophic lateral sclerosis. *Eur Radiol.* 2019;29:4266-4275.
10. Schreiber S, Schreiber F, Debska-Vielhaber G, et al. Differential involvement of forearm muscles in ALS does not relate to sonographic structural nerve alterations. *Clin Neurophysiol.* 2018;129:1438-1443.
11. Brooks BR, Miller RG, Swash M, Munsat TL. El Escorial revisited: revised criteria for the diagnosis of amyotrophic lateral sclerosis. *Amyotroph Lateral Scler.* 2000;1:293-299.
12. Brooks BR. El Escorial world Federation of Neurology criteria for the diagnosis of amyotrophic lateral sclerosis. *J Neurol Sci.* 1994;124:96-107.

13. Joint Task Force of the EFNS and the PNS. European Federation of Neurological Societies/Peripheral Nerve Society guideline on management of paraproteinemic demyelinating neuropathies. Report of a joint task force of the European Federation of Neurological Societies and the Peripheral Nerve Society—first revision. *J Peripher Nerv Syst*. 2010;15:185-195.
14. Rajabally YA, Nicolas G, Piéret F, Bouche P, van den Bergh PYK. Validity of diagnostic criteria for chronic inflammatory demyelinating polyneuropathy: a multicentre European study. *J Neurol Neurosurg Psychiatry*. 2009;80:1364-1368.
15. Chio A, Calvo A, Moglia C, Mazzini L, Mora G. Phenotypic heterogeneity of amyotrophic lateral sclerosis: a population based study. *J Neurol Neurosurg Psychiatry*. 2011;82:740-746.
16. Cedarbaum JM, Stambler N, Malta E, et al. The ALSFRS-R: a revised ALS functional rating scale that incorporates assessments of respiratory function. *J Neurol Sci*. 1999;169:13-21.
17. Yang X, Tridandapani S, Beitler JJ, et al. Ultrasound GLCM texture analysis of radiation-induced parotid-gland injury in head-and-neck cancer radiotherapy: an in vivo study of late toxicity. *Med Phys*. 2012;39:5732-5739.
18. Haralick RM, Shanmugam K, Dinstein I. Textural features for image classification. *IEEE Trans Syst Man Cybern*. 1973;SMC-3:610-621.
19. Brill NA, Tyler DJ. Quantification of human upper extremity nerves and fascicular anatomy. *Muscle Nerve*. 2017;56:463-471.
20. Tang X. Texture information in run-length matrices. *IEEE Trans Image Proc*. 1998;7:1602-1609.
21. Chu A, Sehgal CM, Greenleaf JF. Use of gray value distribution of run lengths for texture analysis. *Pattern Recogn Lett*. 1990;11:415-419.
22. Amadasun M, King R. Textural features corresponding to textural properties. *IEEE Trans Syst Man Cybern*. 1989;19:1264-1274.
23. Vallières M, Freeman CR, Skamene SR, El Naqa I. A radiomics model from joint FDG-PET and MRI texture features for the prediction of lung metastases in soft-tissue sarcomas of the extremities. *Phys Med Biol*. 2015;60:5471-5496.
24. Brysbaert M, Stevens M. Power analysis and effect size in mixed effects models: a tutorial. *J Cogn*. 2018;1:9.
25. Diedenhofen B, Musch J. Cocor: a comprehensive solution for the statistical comparison of correlations. *PLoS One*. 2015;10:e0121945.
26. Schreiber S, Debska-Vielhaber G, Abdulla S, et al. Peripheral nerve atrophy together with higher cerebrospinal fluid progranulin indicate axonal damage in amyotrophic lateral sclerosis. *Muscle Nerve*. 2018;57:273-278.
27. Hobson-Webb LD, Simmons Z. Ultrasound in the diagnosis and monitoring of amyotrophic lateral sclerosis: a review. *Muscle Nerve*. 2019;60:114-123.
28. Atsumi T, Miyatake T. Morphometry of the degenerative process in the hypoglossal nerves in amyotrophic lateral sclerosis. *Acta Neuropathol*. 1987;73:25-31.
29. Bradley WG, Good P, Rasool CG, Adelman LS. Morphometric and biochemical studies of peripheral nerves in amyotrophic lateral sclerosis. *Ann Neurol*. 1983;14:267-277.
30. Silvestri E, Martinoli C, Derchi LE, Bertolotto M, Chiaramondia M, Rosenberg I. Echotexture of peripheral nerves: correlation between US and histologic findings and criteria to differentiate tendons. *Radiology*. 1995;197:291-296.
31. Jongbloed BA, Haakma W, Goedee HS, et al. Comparative study of peripheral nerve MRI and ultrasound in multifocal motor neuropathy and amyotrophic lateral sclerosis. *Muscle Nerve*. 2016;54:1133-1135.
32. Schreiber S, Schreiber F, Garz C, et al. Toward in vivo determination of peripheral nervous system immune activity in amyotrophic lateral sclerosis. *Muscle Nerve*. 2019;59:567-576.
33. Martínez-Payá JJ, Ríos-Díaz J, Del Baño-Aledo ME, Tembl-Ferrairó JI, Vazquez-Costa JF, Medina-Mirapeix F. Quantitative muscle ultrasonography using textural analysis in amyotrophic lateral sclerosis. *Ultrason Imaging*. 2017;39(6):357–368.
34. Martini R, Toyka KV. Immune-mediated components of hereditary demyelinating neuropathies: lessons from animal models and patients. *Lancet Neurol*. 2004;3:457-465.
35. Padua L, Granata G, Sabatelli M, et al. Heterogeneity of root and nerve ultrasound pattern in CIDP patients. *Clin Neurophysiol*. 2014;125:160-165.
36. Härtig F, Ross M, Dammeier NM, et al. Nerve ultrasound predicts treatment response in chronic inflammatory demyelinating polyradiculoneuropathy—a prospective follow-up. *Neurotherapeutics*. 2018;15:439-451.

SUPPORTING INFORMATION

Additional supporting information may be found online in the Supporting Information section at the end of this article.

How to cite this article: Schreiber F, Garz C, Heinze H-J, Petri S, Vielhaber S, Schreiber S. Textural markers of ultrasonographic nerve alterations in amyotrophic lateral sclerosis. *Muscle & Nerve*. 2020;62:601–610. https://doi.org/10.1002/mus.27043